SIMULATION OF FORMATION OF COLD DRAWN SQUARE PRESSURE TUBE OF ZIRCONIUM NIOBIUM [ZR-NB] ALLOY FOR BOILING WATER NUCLEAR REACTORS – A CASE STUDY

Ameya J. More, Abhijit P. Deokule, Niraj C. Deobhankar
Homi Bhabha National Institute, Mumbai, INDIA-400085
E-mail of corresponding author: abhijit.deokule1986@gmail.com

ABSTRACT

Boiling Water Reactors utilize Zirconium-Niobium (Zr-Nb) pressure tubes. These tubes serve the purpose of supporting rod bundles as well as providing passage for coolant. The thermal neutron absorption cross section of Zr-Nb is almost negligible compared to Uranium for thermal neutrons. Higher structural strength is the main advantages of square tube over circular tube; higher heat transfer area is an additional advantage. Ordinarily circular tubes and square tubes are formed by extrusion hot Zr-Nb alloy. Our aim was to find out an alternative manufacturing technique for mass production of Zr-Nb square tube. Recent advances in finite element method have led us to simulate and study cold drawing process. Here, study is carried out to simulate the process of formation of square tube from circular tube by cold drawing process, using finite element analysis.

INTRODUCTION

The use of circular tubes in energy absorbing systems is an attractive topic and has been discussed by several authors [1–5]. The circular tube compressed between two rigid, parallel plates has also been discussed [6–10] to explore the characteristics of collapse occurrence. Surely, there seems to be lack in attempts to analyze manufacturing of square cross section tube by cold drawing from circular cross section.

Zr-Nb alloy is an HCP material and cannot be simply drawn by using cold drawing process for higher elongations. This limitation makes cold pilgering a preferable choice over cold drawing. Still keeping the area reduction as a limiting factor of cold drawn tube the tooling for cold drawing was designed. The elongation of the tube was kept limited up to five percents only. This reduces length of the tube after cold drawing to a remarkably low value but it reduces the stresses induced in the cold draw tooling and drawing load. Metal forming processes utilize large forces on to the work material for manufacturing the desired shape of the product. Determination of the applied force is of utmost importance in metal forming processes, as it influences residual stresses and plastic deformation in final product. Residual stresses along with postulated defects in any component affect structural integrity of the component. Deformations influences failure criterion of the component. Hence, in this study an attempt has been made to analyze residual stress distribution and deformation in the component.

BASIC THEORY

Tooling Design

Fig.1 shows the mechanism of squaring of circular tube by cold drawing. In cold drawing, force is applied by the die in inward direction. Plug is used to support the tube and to provide essential thickness reduction during cold drawing. The size of the mother tube is calculated by computing the equivalent diameter of the square tube and dividing it by area reduction. The corners of the plug are chamfered to avoid the contact between the tube and the plug and to keep the stresses induced to lower permissible value. Fig.2 shows essential parts required for cold drawing of tube. For this particular case study the square tube with an arbitrary size 120 X 120 mm with 5mm thickness was chosen. Diameter of the mother tube (D) and thickness (t) was determined by applying area reduction on the equivalent average diameter of the product tube. This equivalent average diameter (D*) was calculated by using relation (1)

$$D^* = \frac{\text{perimeter of the product tube}}{\pi} \tag{1}$$

$$D = \sqrt{\frac{4\,(D^* - t)(t)}{(0.95)}} \tag{2}$$

Area reduction is limited to five percents of the mother tube so mother tube diameter is calculated by considering the area reduction in the product tube. Thus diameter of the mother tube (D) is given by relation (2) as shown above.

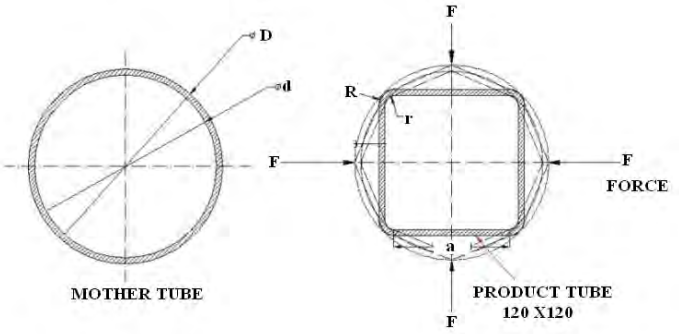

Fig.1: Conversion of Round Tube into Square Tube

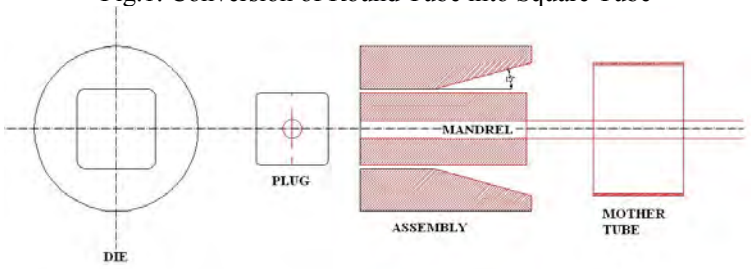

Fig.2: Tooling for cold drawing

Variational principle

The updated Lagrangian formulation (ULF), pioneered by McMeeking and Rice [12], is more suitable for describing the incremental characteristics of plastic flow. For each time instant, the reference state is updated to coincide with the current state of deformation. The rate equation of virtual work in updated Lagrangian form using the Jaumann rate of Cauchy stress proposed by McMeeking and Rice [12] can be expressed as

$$\int_V \left(\sigma_{ij}^J - 2\sigma_{ik}\dot{\varepsilon}_{kj}\right)\delta\dot{\varepsilon}_{ij}dV + \int_V \sigma_{jk}L_{ik}\delta L_{ij}dV = \int_{Sf} \dot{f}_i \delta\, v_i \delta S \tag{3}$$

Where $\sigma_{ij}^J = (\dot{\sigma}_{ij} + \sigma_{kj} \cdot w_{ik} - w_{ik} \cdot \sigma_{kj})$ is the Jaumann rate of Cauchy stress $\sigma_{ij,}$ $\dot{\varepsilon}_{ij}$ is the strain rate, $L_{ij}=(\partial v_i/\partial X_j)$ denotes the velocity gradient, X_j is the spatial fixed Cartesian coordinate, v_i is the velocity, $\dot{f}_i$ is the rate of nominal traction and V and S_f are the material volume and the surface on which traction is prescribed.

Constitutive model

When elastic loading or plastic unloading is encountered, the elastic effect has to be considered in FE simulation. In the present work the assumptions made for elasto-plastic constitutive relation are the following

1. Elastic behavior: isotropic and linear elasticity with small strain;
2. Plastic behavior: rate independent, isotropic strain hardening, Von Mises yield function and associative flow rule.

The constitutive relation which incorporates small elastic-finite plastic deformation behavior, is written as

$$\sigma_{ij}^J = \frac{E}{1+\nu}\left[\delta_{ik}\delta_{jl} + \frac{\nu}{1-2\nu}\delta_{ij}\delta_{kl} - \frac{3\alpha\left(\frac{E}{1+\nu}\right)\sigma'_{ij}\,\sigma'_{kl}}{2\bar{\sigma}^2\left(\frac{2}{3}H' + \frac{E}{1+\nu}\right)}\right]\dot{\varepsilon}_{kl} \tag{4}$$

Where σ'_{ij} is deviatoric part of the σ'_{ij} , H' is the rate of strain hardening, E is the elastic modulus, υ is the Poisson's ratio, δij is the Kronecker delta, equivalent stress $\bar{\sigma}$ obeys the Von Mises yield function, and α takes unity for the plastic state and zero for the elastic state or the unloading.

The relationship of equivalent stress $\bar{\sigma}$ and equivalent plastic strain $\bar{\varepsilon}_p$ of the material is represented by an n-power law of the form

$$\bar{\sigma} = K\,\bar{\varepsilon}_p^n \tag{5}$$

In order to model the hardening behavior in which *n* denotes the strain hardening exponent and *K* is a material constant.

Yield Criterion

The yield criterion determines the stress level at which yielding is initiated. For multi-component stresses, this is represented as a function of the individual components, f ({σ}), which can be interpreted as equivalent stress σ_e,

$$\sigma_e = f(\{\sigma\}) \tag{6}$$

If the equivalent stress computed using elastic properties exceeds the material yield, then plastic straining must occur. Plastic strains reduce the stress state so that it satisfies the yield criterion, Equation (6). Based on the theory the plastic strain increment is readily calculated. The hardening rule states that the yield criterion changes with work hardening and with kinematic hardening. Incorporating these dependencies into Equation (6), and recasting it into the following form

$$F(\{\sigma\}, k, \{\alpha\}) = 0 \tag{7}$$

κ and {α} are termed internal or state variables. Specifically, the plastic work is the sum of the plastic work done over the history of loading, F is the yield criterion.

$$\{d\sigma\} = [D]\{d\varepsilon^{el}\} \tag{8}$$

$$\{d\varepsilon^{el}\} = \{d\varepsilon\} - \{d\varepsilon^{pl}\} \tag{9}$$

Since the total strain increment can be divided into an elastic and plastic part.

$$\lambda = \frac{\left\{\frac{\partial F}{\partial \sigma}\right\}[M][D]\{d\varepsilon\}}{-\left\{\frac{\partial F}{\partial k}\right\}\{\sigma\}^T[M]\left\{\frac{\partial Q}{\partial \sigma}\right\} - C\left\{\frac{\partial F}{\partial \alpha}\right\}[M][D]\left\{\frac{\partial Q}{\partial \sigma}\right\} + \left\{\frac{\partial F}{\partial \sigma}\right\}[M][D]\left\{\frac{\partial Q}{\partial \sigma}\right\}} \tag{10}$$

Where,

$$[M] = \begin{bmatrix} 1 & 0 & 0 & 0 & 0 & 0 \\ 0 & 1 & 0 & 0 & 0 & 0 \\ 0 & 0 & 1 & 0 & 0 & 0 \\ 0 & 0 & 0 & 2 & 0 & 0 \\ 0 & 0 & 0 & 0 & 2 & 0 \\ 0 & 0 & 0 & 0 & 0 & 2 \end{bmatrix} \tag{11}$$

F =Yield criterion, Q = plastic potential, [D] = stress strain matrix.

The size of the plastic strain increment is therefore related to the total increment in strain, the current stress state, and the specific forms of the yield and potential surfaces. The plastic strain increment is then computed using equation (12)

$$\{d\varepsilon^{pl}\} = \lambda \{\partial Q | \partial \sigma\} \tag{12}$$

The elastoplastic stress-strain matrix is derived from the local Newton-Raphson iteration scheme used [4]. It is therefore the consistent (or algorithmic) tangent. If the flow rule is not associative (F ≠ Q), then the tangent is unsymmetrical. To preserve the symmetry of the matrix, for analyses with a no associative flow rule (Drucker-Prager only), the matrix is evaluated using F only and again with Q only and the two matrices averaged.Fig.3 shows the tangent modulus calculated at various places along the multilinear isotropic curve. This tangent modulus was used to calculate stiffness matrix as the deformation progressed.

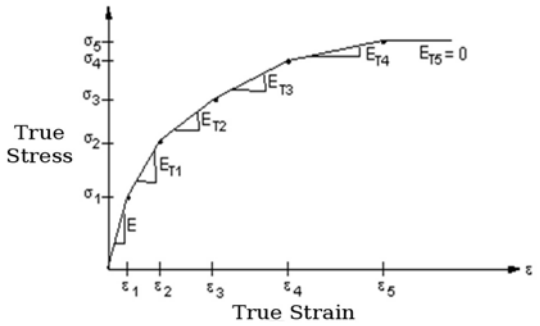

Fig. 3: Uniaxial Behaviors for Multilinear Isotropic Hardening

Finite element discretization and model

As the principle of virtual work rate equation and the constitutive relation are linear equations of rates, these can be replaced by increments defined with respect to any continuously increasing measure, such as the tool displacement increment. And all rate quantities can be replaced by incremental quantities. Performing a standard procedure of finite-element discretization, Eq. 3 yields a system of algebraic equation, which in matrix form can be represented by

$$[\mathrm{K}]\{\Delta u\} = \{\Delta \mathrm{F}\} \tag{13}$$

$$[\mathrm{K}] = \sum_{<e>} \int_{V\langle e\rangle} [B]^T ([D^{e\,p}] - [Q])\,[B] dV + \sum_{<e>} \int_{V<e>} [E]^T\,[Z][E] dV \tag{14}$$

In these equations, [K] is the global elasto-plastic tangent stiffness matrix which is regarded as constant within each incremental step, {Δu} denotes the nodal displacement increment, {ΔF} denotes the prescribed nodal force increment, [D^{ep}] is the elemental elasto-plastic constitutive matrix, and [B] and [E] denote the strain matrix and the velocity gradient matrix, respectively.[Q] and [Z] are defined as stress correction matrices due to the current stress states at any stage of deformation.

Formulation of friction condition

The friction condition in the contact zone between work-piece and tools plays an important role in the deformation process. A modified Coulomb friction law proposed by Oden and Pries [13] is adopted to describe the friction state. Two contact friction states such as sticking and sliding can be treated well by making use of this analytical friction law in an incremental way. The increment of tangential force Δf_l, the direction of which coincides with the sliding direction, is obtained by the adopted friction law,

$$\Delta f_l = \pm \mu\, \Delta f_n \Phi(\Delta u_l^{rel}) \tag{15}$$

in which Δf_n denoted as the increment of normal force, Φ ($\Delta u_l^{\mathrm{rel}}$) adopted as *tanh* ($3\Delta u_l^{\mathrm{rel}}$/ *vcri*) [13] is an analytical hyperbolic function which is used to substitute for the discontinuity of sliding and sticking involved in some friction law such as the Coulomb friction law, *vcri* denotes the limit displacement increment for quasi-sticking and $\Delta u_l^{\mathrm{rel}}$ is the sliding displacement increment relative to the tube movement,

$$\Delta u_l^{rel} = \Delta u_l - \Delta U \sin\theta \tag{16}$$

in which θ is the angle between the *l*-axis and the horizontal axis, Δu_l is the tangential displacement increment of the contact node and ΔU is the tool displacement increment. The increment of nodal force $\vec{\mathrm{F}}$ acting on the contact node is written as

$$\Delta \vec{\mathrm{F}} = \Delta f_l \vec{l} + \Delta f_{\mathrm{n}} \vec{\mathrm{n}} \tag{17}$$

in which, $\vec{\mathrm{n}}$ is the outward vector normal to the tool surface and $\vec{l}$ is perpendicular to $\vec{\mathrm{n}}$.

The global stiffness matrix with respect to the contact node by

$$\begin{bmatrix} k & \cdots & \cdots \\ \cdots & k_{11} & k_{12} \\ \cdots & k_{21} & k_{22} \end{bmatrix} \begin{Bmatrix} \cdots \\ \Delta u_l^i \\ \Delta \bar{u}_l^i \end{Bmatrix} = \begin{Bmatrix} \cdots \\ \Delta f_l^{i-1} \\ \Delta f_n^i \end{Bmatrix} \tag{18}$$

in which $\Delta\bar{u}_n$ is a prescribed displacement increment of the contact node in the normal direction of contact boundary, equal to $\Delta U \cdot \cos\theta$, i denotes the current incremental step and i−1 denotes the previous incremental step. In the solution scheme, the increment of friction force of contact node is calculated iteratively.

Weighting factor for the increment of each loading step

During each increment, the material is referred to its configuration at the beginning of the increment (updated Lagrangian scheme). The contact and separation conditions of nodes and the state of elements must remain invariable during the increment. In order to satisfy this requirement and to assure the accuracy of this explicit integration scheme (static explicit formulation), the weighting factor proposed by Yamada et al. [11] is used to treat the elasto-plastic and contact-separation problems to choose the size of the increment to keep linear relation. The size of each loading step is determined by the smallest value of the five r-values. The above is proved valid in the first order theory. More detailed information of weighting factor can be found in literature [14].

Unloading process

In order to know the final shape or the spring back behavior, the unloading process is executed by assuming that all elements are reset to be elastic. The force of the contact node is reversed to become the prescribed force boundary condition. All tools are removed for the elastic unloading procedure.

Summary of solution procedure

The algorithm for simulating the squaring process of circular tube is summarized as following:

1. Set up the initial conditions, and prescribe the boundary conditions and a fictitious tube displacement increment Δu at the beginning of the increment.
2. Calculate stiffness matrix $[K]$ and solve the stiffness equation for a fictitious solution $\{\Delta u\} = [K]^{-1}\{\Delta F\}$ correspondent to the previous tube displacement.
3. A "real" solution $u_i = u_{i-1} + \Delta u_i$ that validates each condition is used to update geometry of deformed tube, displacements, stresses, yield limit of each element, and boundary conditions of each contact element.
4. If the prescribed tube displacement is reached, then the unloading procedure is executed and output the total results; otherwise go to step 2.

GEOMETRIC MODELING AND FEM FORMULATION

The geometric modeling was carried out for quarter section of the problem. The initial tube was a circular and the final product was a square tube. Tangential continuity was kept throughout the die. The plug was a square plug which has a functioning of providing inner support to the tube.Fig.4 (a, b, c) shows the geometry of the quarter section of the tube, die and plug.Fig.4 (d) shows the complete assembly of the quarter section of the cold drawn tube. To simulate this process in FEM the symmetry of the model was considered to reduce the complexity in the calculations. This has also reduced computer processing time and allocated memory space. Plasticity theory provides a mathematical relationship that characterizes the elastoplastic response of materials. There are three ingredients in the rate-independent plasticity theory: the yield criterion, flow rule and the hardening rule. These will be discussed in detail subsequently.

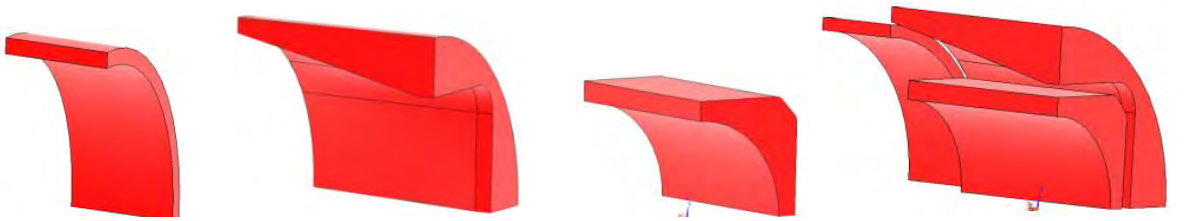

a) Tube *b) Die* *c) Plug* *d) Assembly of quarter model*

Fig.4: Geometric model of the quarter section of the cold draw tooling.

There is symmetry in the die and plug and also in tube. Quarter model was taken for FEM simulation. It was modeled and meshed. Fig. 5 shows meshed quarter model of die, plug and tube all were meshed by using solid 95 elements. The geometry of the die was modeled so that tangential continuity was maintained throughout the geometry of the die. The die and the plug materials were selected as D-3 tool steel and the deformation in the die and the plug was neglected. It was assumed that the deformation in the die and the plug material is below yield point due to its higher value of the Young's modulus of the D-3 material. The tube is deformed in the elastoplastic region and true stress- strain values were assigned to the element. Fig. 6 shows the multilinear isotropic properties for Zirconium Niobium alloy [Zr-2.5%Nb].These multilinear isotropic true stress strain values were taken from experimental values in true stress strain region of the curve.

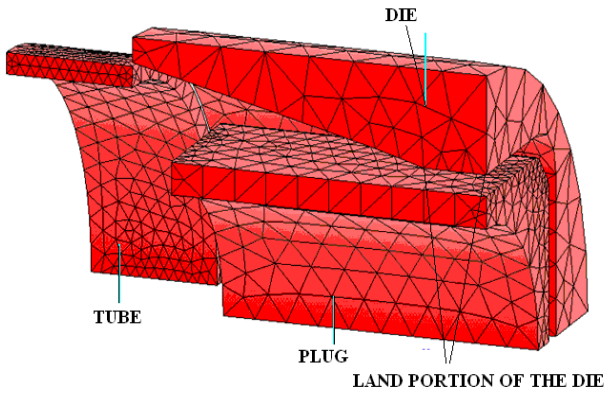

Fig. 5: Meshed quarter model of cold drawing assembly

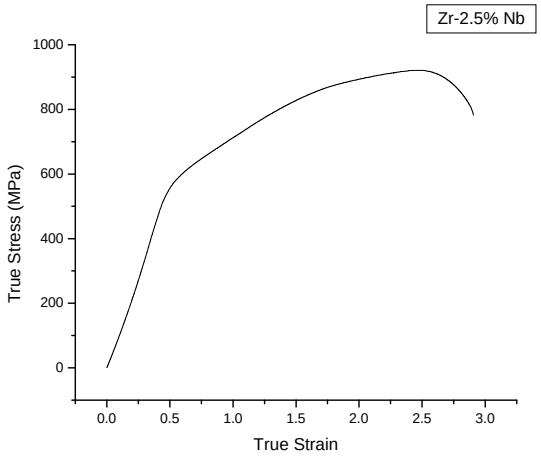

Fig. 6: Multilinear Isotropic Properties for Zr-2.5Nb

Boundary Conditions

In accordance with the phenomenon of cold drawing nodal displacement of die and plug was kept zero in all directions. Since Die and plug were considered as rigid surfaces so stress distribution in die or plug was neglected. Max. Permissible (desired) displacement of the tube in the direction of cold drawing is 1.5 times that of the existing tube length size. Contacting surfaces were assigned node to node contact with coefficient of friction pairs μ=0.1. Fig.7 shows the contact conditions between die, tube and plug. The contact was made so that the normal drawn from the nodes are directed towards each other and will get engaged during the process of cold drawing.

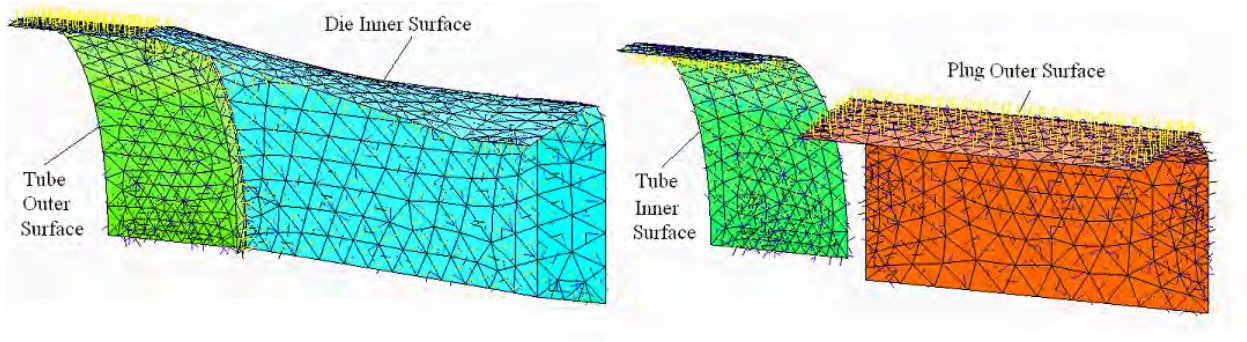

(a) Die Inner surface and tube outer surface (b)Tube inner surface and plug outer surface

Fig.7: Contact conditions

SIMULATION

In this simulation we have assigned the displacement on the tube nodes while die and plug both were kept stationary. The simulation involves material non linearity as well as geometric non linearity so the iterative solver was used. The finite element was chosen and then time step at the end of load step was assigned an arbitrarily fixed value. Minimum time step and maximum time step was given a value of 0.1 and 1.5 respectively. Condition for convergence was kept that norm of the matrix should be less than unity. The simulation is carried out to observe the geometry of cold drawn tube and stresses induced during the rate independent plastic deformation. The cold drawing induces spring back effect due to large plastic deformation. However if the length of the land portion of the die is kept sufficiently large the spring back effect in the tube can be limited to a lower permissible value.

NUMERICAL RESULTS

Large strain static analysis is carried out and results are obtained after complete solution of the problem with the applied boundary conditions. The geometry of cold drawn square tube is without any concavity or convexity which comes through plastic deformation. Von Mises stresses were calculated and plotted in the Fig.8. The maximum value of Von Mises stress in the tube was less than the ultimate tensile stress. Equivalent plastic strain per unit volume is higher at the corner than the remaining tube as shown in Fig.9. Hence, Principal stresses at a particular corner node and varying with respect to time are plotted in Fig.10. Similarly Von Mises stresses for the same node varying with respect to time are plotted in Fig.11, whereas equivalent plastic strain for the same node point and varying with respect to time is plotted in Fig.12.

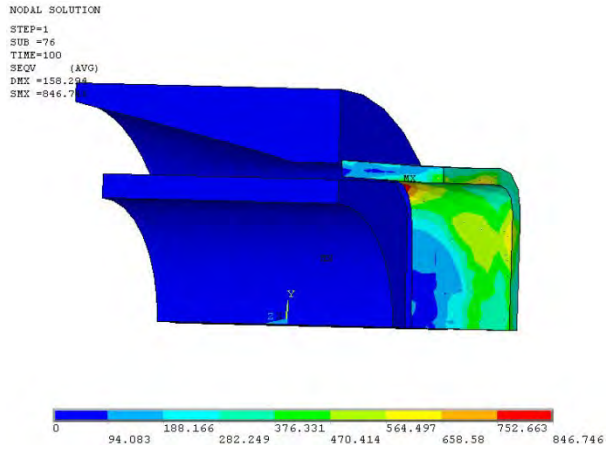

Fig.8: Von Mises stress distribution

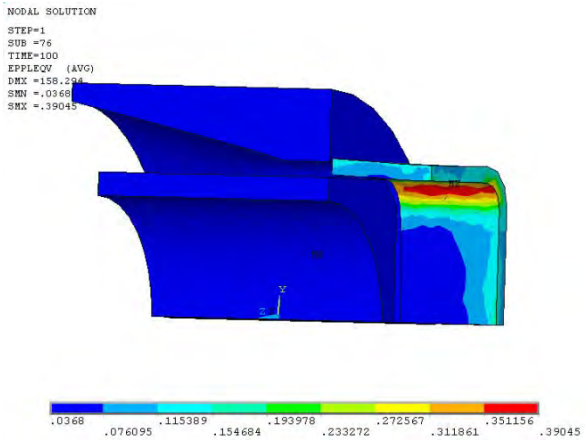

Fig.9: Equivalent plastic strain

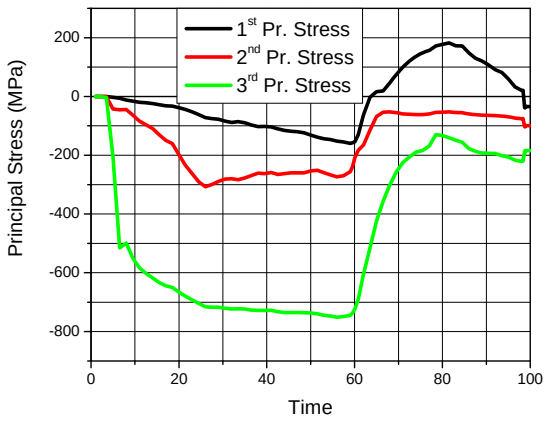

Fig.10: Principal Stresses

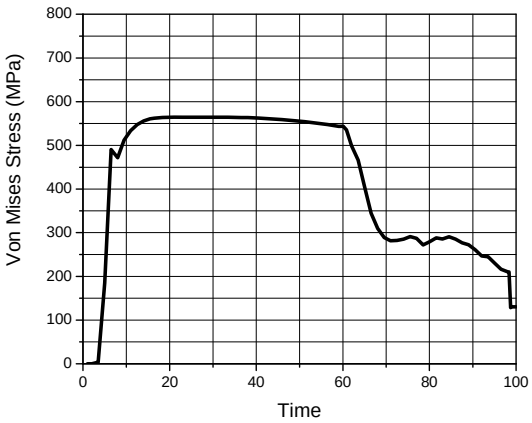

Fig.11: Von Mises Stress

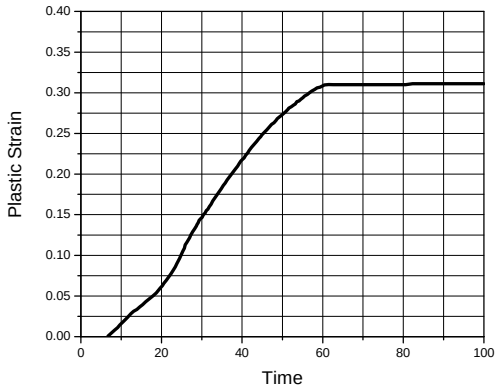

Fig.12: Equivalent Plastic Strain

CONCLUSION

Zirconium niobium [Zr-2.5%Nb] square tube can be formed by cold drawing process without spring back effect if the area reduction in the tube is limited to a smaller value up to five percents of original area of the tube. Also the amount of residual stresses induced in the tube was confined to a lower value than the ultimate tensile strength which indicates that material cannot fail during the actual trial. Geometry of the square tube shows that if the land portion of the plug and die is sufficiently long the spring back effect on the edges of the square tube formed is negligible.

REFERENCES

[1] Carney JF III, Austin CD, Reid SR (1983) Modeling of steel tube vehicular crash cushion. ASCE Transport Eng. 109(3):331–346.
[2] Reid SR, Drew SLK, Carney JF III (1983) Energy absorbing capacities of braced metal tubes. Int. J. Mech. Sci. 25(9–10):649–667.
[3] Watson AR, Reid SR, Johnson W, Thomas SG (1976) Large deformations of thin-walled circular tubes under transverse loading-II. Int. J. Mech. Sci. 18:387–397.
[4] Watson AR, Reid SR, Johnson W (1976) Large deformations of thin walled circular tubes under transverse loading-III. Int. J. Mech. Sci. 18:501–509.
[5] Johnson W, Reid SR (1977) The compression of crossed layers of thin tubes. Int. J. Mech. Sci. 19:423–437.
[6] Mutchler LD (1960) Energy absorption of aluminum tubing. Trans. ASME J. Appl. Mech. 27:740–743.
[7] DeRuntz JA, Hodge PG (1963) Crushing of a tube between rigid plates. Trans. ASME J. Appl. Mech .
[8] Johnson W (1972) Impact strength of material. Arnold, London.
[9] Reid SR, Reddy TY (1978) Effect of strain hardening on the lateral compression of tubes between rigid plates. Int. J. Solid. Struct. 14: 213–225.
[10] Gotoh M, Shibada Y (1989) Elasto-plastic finite element analysis for one and two dimensions of lateral compression of tube. Spring Proc. Plastic Working. Cho-Fu, Tokyo, 18 May 1989, pp 571–574.
[11] Yamada Y, Yoshimura N, Sakurai T (1968) Plastic stress-strain matrix and its application for the solution of elastic-plastic problems by the finite element method. Int. J. Mech. Sci. 10:343–354.
[12] McMeeking RM, Rice JR (1975) Finite element formulations for problems of large elastic-plastic deformation. Int. J. Solid Struct. 11:601–616.
[13] Oden JT, Pries EB (1983) Nonlocal and nonlinear friction law and variational principles for contact problems in elasticity. Trans. ASME J Appl. Mech. 50:67–76.
[14] Leu DK (1996) Finite-element simulation of hole-flanging process of circular sheets of anisotropic materials. Int. J. Mech. Sci. 38(8–9): 917–933.
[15] Juneja B.L. “Introduction to metal forming technology” New age publication, 2000.
[16] Daw- Kwei Leu “FE simulation of the squaring of circular tube “Journal of Adv. Mfg. tech. (2005).
[17] Simo, J. C. "Consistent Tangent Operators for Rate-Independent Elastoplasticity", Computer Methods in Appl. Mech. and Eng., Vol. 48, pp. 101-118 (1985).